

Estimate of the Cutoff Errors in the Ewald Summation for Dipolar Systems

Zuowei Wang, Christian Holm

Max-Planck-Institut für Polymerforschung, Ackermannweg 10, D-55128 Mainz, Germany

(November 7, 2018)

Abstract

Theoretical estimates for the cutoff errors in the Ewald summation method for dipolar systems are derived. Absolute errors in the total energy, forces and torques, both for the real and reciprocal space parts, are considered. The applicability of the estimates is tested and confirmed in several numerical examples. We demonstrate that these estimates can be used easily in determining the optimal parameters of the dipolar Ewald summation in the sense that they minimize the computation time for a predefined, user set, accuracy.

PACS: 02.70.Ns Molecular dynamics and particle methods; 87.15.Aa Theory and modeling; computer simulation; 61.20.Ja Computer simulation of liquid structure; 83.80.Gv Electro- and magnetorheological fluids,

I. INTRODUCTION

Computer simulations are becoming more and more important in the study of complex systems. Among them many of the most interesting systems are charged systems, and as such naturally dominated by long range interactions. This is certainly the case for almost all biological systems where the electrostatic interactions play a dominant role¹, but there is also a wealth of technological important substances such as polyelectrolytes, where the charged nature is one of the key ingredient for their functionality². The electrostatic interactions can be of monopolar origin, like interactions between proteins, DNA, or charged membranes, but also of dipolar nature, because all biological tissues contain water, which is a dipolar substance. The simultaneous appearance of dipoles and monopoles is of great importance, for example, for protein folding simulations³. Dipolar interactions can also be of technological importance, for example in the application of so called ferrofluids, which are basically dispersed magnetic particles⁴. However, computer simulations of long range interactions in periodic boundary conditions are notoriously difficult to handle, and possess an unfavorable scaling with the amount of particles involved. The most often used method to compute the interactions relies on the famous Ewald sum⁵. In the simplest implementations the involved computation time grows like N^2 , or at best like $N^{3/2}$, if the cutoff is optimally varied with the splitting parameter⁶. The use of fast Fourier transformations (FFT) can further reduce the scaling to basically $N \cdot \log N$. There have been quite a number of advances in the application of these so-called particle-mesh-Ewald techniques for Coulomb systems over the last few years⁷⁻¹¹. An important aspect of all algorithms is the tuning in the sense of speed at well controlled errors. All algorithms have parameters such as the real space cutoff r_c , the reciprocal space cutoff k_c , the splitting parameter α , and for the mesh based methods there are even more. To find the optimal combination and at the same time control the systematic error is a formidable task, and cannot efficiently be achieved by trial and error. For the simulations of point charges, there have been reliable error estimates published for the standard Ewald summation¹², and for the mesh Ewald methods PME¹³ and P3M¹⁴. For the dipolar Ewald summation, there has been just an estimate given for the energy in real-space in Ref. 12. For molecular dynamics (MD) simulations of dipolar systems, however, we need to know the errors for the forces and the torques. In this article we give a reliable error estimate for the energy, for the forces, and for the torques, when computed via the standard Ewald sum. We will show the applicability of these estimates by comparing them to well specified systems. Moreover we will give a detailed discussion on the optimization of the parameters, which will lead to the most efficient parameters for a predefined error in each observable quantity. This can all be done prior to the actual simulation, ensuring thus optimal performance at optimally controlled errors.

The article is organized as follows: In Sec. II we briefly review the important formulas of the Ewald summation for dipolar systems. The theoretical estimates of the cut-off errors in the Ewald sum are derived in Sec. III. In Sec. IV the estimates are compared with numerical accuracy measurements for specified model systems, and they are found to be very precise. The use of the estimates in determining the optimal parameters and their application to an inhomogeneous system is discussed in Sec. V and VI, respectively. Finally we end with some conclusions in Sec. VII.

II. THE EWALD SUMMATION

Consider a system of N particles with a point-dipole $\boldsymbol{\mu}_i$ at their center position \mathbf{r}_i in a cubic simulation box of length L . If periodic boundary conditions are applied, the total electrostatic energy of the box is given by

$$U = \frac{1}{2} \sum_{i=1}^N \sum_{j=1}^N \sum'_{\mathbf{n} \in \mathbb{Z}^3} \left\{ \frac{\boldsymbol{\mu}_i \cdot \boldsymbol{\mu}_j}{|\mathbf{r}_{ij} + \mathbf{n}|^3} - \frac{3[\boldsymbol{\mu}_i \cdot (\mathbf{r}_{ij} + \mathbf{n})][\boldsymbol{\mu}_j \cdot (\mathbf{r}_{ij} + \mathbf{n})]}{|\mathbf{r}_{ij} + \mathbf{n}|^5} \right\}. \quad (1)$$

where $\mathbf{r}_{ij} = \mathbf{r}_i - \mathbf{r}_j$. The sum over \mathbf{n} is over all simple cubic lattice points, $\mathbf{n} = (n_x L, n_y L, n_z L)$ with n_x, n_y, n_z integers. The prime indicates that the $i = j$ term must be omitted for $\mathbf{n} = 0$. The slowly decaying long range part of the dipolar potential renders the straightforward summation of Eqn.(1) impracticable. The Ewald method provides an efficient way of calculating U , which splits the problem into two absolutely and rapidly convergent parts, one in real space and one in reciprocal space. The details of the method are discussed in Refs. 5,6,15,16, here we only give the final expressions

$$U = U^{(r)} + U^{(k)} + U^{(self)} + U^{(surf)}, \quad (2)$$

where the real-space $U^{(r)}$, the k-space (reciprocal-space) $U^{(k)}$, the self $U^{(self)}$ and the surface $U^{(surf)}$ contributions are respectively given by:

$$U^{(r)} = \frac{1}{2} \sum_{i=1}^N \sum_{j=1}^N \sum'_{\mathbf{n} \in \mathbb{Z}^3} \left\{ (\boldsymbol{\mu}_i \cdot \boldsymbol{\mu}_j) B(|\mathbf{r}_{ij} + \mathbf{n}|) - [\boldsymbol{\mu}_i \cdot (\mathbf{r}_{ij} + \mathbf{n})][\boldsymbol{\mu}_j \cdot (\mathbf{r}_{ij} + \mathbf{n})] C(|\mathbf{r}_{ij} + \mathbf{n}|) \right\}, \quad (3)$$

$$U^{(k)} = \frac{1}{2L^3} \sum_{\mathbf{k} \in \mathbb{Z}^3, \mathbf{k} \neq 0} \frac{4\pi}{k^2} \exp[-(\pi k/\alpha L)^2] \sum_{i=1}^N \sum_{j=1}^N (\boldsymbol{\mu}_i \cdot \mathbf{k})(\boldsymbol{\mu}_j \cdot \mathbf{k}) \exp(2\pi i \mathbf{k} \cdot \mathbf{r}_{ij}/L), \quad (4)$$

$$U^{(self)} = -\frac{2\alpha^3}{3\sqrt{\pi}} \sum_{i=1}^N \mu_i^2, \quad (5)$$

$$U^{(surf)} = \frac{2\pi}{(2\epsilon' + 1)L^3} \sum_{i=1}^N \sum_{j=1}^N \boldsymbol{\mu}_i \cdot \boldsymbol{\mu}_j. \quad (6)$$

Here the sums over i and j are for the particles in the central box and

$$B(r) = [\operatorname{erfc}(\alpha r) + (2\alpha r/\sqrt{\pi}) \exp(-\alpha^2 r^2)]/r^3, \quad (7)$$

$$C(r) = [3\operatorname{erfc}(\alpha r) + (2\alpha r/\sqrt{\pi})(3 + 2\alpha^2 r^2) \exp(-\alpha^2 r^2)]/r^5. \quad (8)$$

The prime on the third sum in Eqn.(3) also denotes that the divergent terms $i = j$ for $\mathbf{n} = 0$ have to be omitted, $\operatorname{erfc}(x) := 2\pi^{-1/2} \int_x^\infty \exp(-t^2) dt$ is the complementary error function. The inverse length α is the splitting parameter of the Ewald summation which should be chosen so as to optimize the performance. The form Eqn.(6) given for the surface correction assumes that the set of the periodic replications of the simulation box tends in a spherical way towards an infinite cluster and that the medium outside this sphere is an uniform

dielectric with dielectric constant $\epsilon'^{15,16}$. The case of a surrounding vacuum corresponds to $\epsilon' = 1$ and the surface term vanishes for the metallic boundary conditions ($\epsilon' = \infty$).

In practical calculations, the infinite sums in Eqns.(3, 4) are truncated by only taking into account distances which are smaller than some real space cutoff r_c and wave vectors with a modulus smaller than some reciprocal space cutoff k_c . If $r_c \leq L/2$, the sum in real space (Eqn.(3)) reduces to the normal minimum image convention. The double sum over particles in $U^{(k)}$ can be replaced by a product of two single sums which is more suitable for numerical calculations.

The force \mathbf{F}_i acting on particle i is obtained by differentiating the potential energy U with respect to \mathbf{r}_i , i.e.,

$$\mathbf{F}_i = -\frac{\partial U}{\partial \mathbf{r}_i} = \mathbf{F}_i^{(r)} + \mathbf{F}_i^{(k)}, \quad (9)$$

with the real-space and k-space contributions given by:

$$\begin{aligned} \mathbf{F}_i^{(r)} = & \sum_{j=1}^N \sum'_{\mathbf{n} \in \mathbb{Z}^3} \left\{ \{(\boldsymbol{\mu}_i \cdot \boldsymbol{\mu}_j)(\mathbf{r}_{ij} + \mathbf{n}) + \boldsymbol{\mu}_i[\boldsymbol{\mu}_j \cdot (\mathbf{r}_{ij} + \mathbf{n})] + [\boldsymbol{\mu}_i \cdot (\mathbf{r}_{ij} + \mathbf{n})]\boldsymbol{\mu}_j\}C(|\mathbf{r}_{ij} + \mathbf{n}|) \right. \\ & \left. - [\boldsymbol{\mu}_i \cdot (\mathbf{r}_{ij} + \mathbf{n})][\boldsymbol{\mu}_j \cdot (\mathbf{r}_{ij} + \mathbf{n})]D(|\mathbf{r}_{ij} + \mathbf{n}|)(\mathbf{r}_{ij} + \mathbf{n}) \right\}, \end{aligned} \quad (10)$$

$$\mathbf{F}_i^{(k)} = \frac{2\pi}{L^4} \sum_{j=1}^N \sum'_{\mathbf{k} \in \mathbb{Z}^3, \mathbf{k} \neq 0} \frac{4\pi\mathbf{k}}{k^2} (\boldsymbol{\mu}_i \cdot \mathbf{k})(\boldsymbol{\mu}_j \cdot \mathbf{k}) \exp[-(\pi k/\alpha L)^2] \sin(2\pi\mathbf{k} \cdot \mathbf{r}_{ij}/L), \quad (11)$$

where

$$D(r) = [15\text{erfc}(\alpha r) + (2\alpha r/\sqrt{\pi})(15 + 10\alpha^2 r^2 + 4\alpha^4 r^4) \exp(-\alpha^2 r^2)]/r^7. \quad (12)$$

Since the self and surface energy terms [Eqns.(5, 6)] are independent of the particle positions, they have no contributions to the force, unlike the Ewald summation for the Coulomb systems where the surface term contributes.

The torque $\boldsymbol{\tau}_i$ acting on particle i is related to the electrostatic field \mathbf{E}_i at the location of this particle,

$$\boldsymbol{\tau}_i = \boldsymbol{\mu}_i \times \mathbf{E}_i = \boldsymbol{\tau}_i^{(r)} + \boldsymbol{\tau}_i^{(k)} + \boldsymbol{\tau}_i^{(surf)}, \quad (13)$$

with

$$\mathbf{E}_i = -\frac{\partial U}{\partial \boldsymbol{\mu}_i}, \quad (14)$$

and thus

$$\boldsymbol{\tau}_i^{(r)} = -\sum_{j=1}^N \sum'_{\mathbf{n} \in \mathbb{Z}^3} \left\{ (\boldsymbol{\mu}_i \times \boldsymbol{\mu}_j)B(|\mathbf{r}_{ij} + \mathbf{n}|) - [\boldsymbol{\mu}_i \times (\mathbf{r}_{ij} + \mathbf{n})][\boldsymbol{\mu}_j \cdot (\mathbf{r}_{ij} + \mathbf{n})]C(|\mathbf{r}_{ij} + \mathbf{n}|) \right\}, \quad (15)$$

$$\boldsymbol{\tau}_i^{(k)} = -\frac{1}{L^3} \sum_{j=1}^N \sum_{\mathbf{k} \in \mathbb{Z}^3, \mathbf{k} \neq 0} \frac{4\pi}{k^2} (\boldsymbol{\mu}_i \times \mathbf{k})(\boldsymbol{\mu}_j \cdot \mathbf{k}) \exp[-(\pi k/\alpha L)^2] \exp(2\pi i \mathbf{k} \cdot \mathbf{r}_{ij}/L), \quad (16)$$

$$\boldsymbol{\tau}_i^{(surf)} = -\frac{4\pi}{(2\epsilon' + 1)L^3} \sum_{j=1}^N \boldsymbol{\mu}_i \times \boldsymbol{\mu}_j. \quad (17)$$

When performing computational simulations, it is important to control the accuracy properly. In molecular dynamics methods the accuracy is generally estimated from the root mean square (rms) error in the forces.^{10,13,14}

$$\Delta F := \sqrt{\frac{1}{N} \sum_{i=1}^N (\Delta \mathbf{F}_i)^2} := \sqrt{\frac{1}{N} \sum_{i=1}^N (\mathbf{F}_i - \mathbf{F}_i^{\text{exa}})^2} \quad (18)$$

where \mathbf{F}_i is the force on particle i calculated by the algorithm under investigation (here the Ewald sum) and $\mathbf{F}_i^{\text{exa}}$ is the *exact* force on that particle. In next section, we will derive estimates for the rms error ΔF caused by cutting off the Ewald summation in real-space and k-space. The similar estimates are also derived for the cutoff errors in the total energy and torques. There are no errors involved in the self and surface contributions (Eqns(5, 6, 17)), because no cutoff operations are applied to them.

III. EXPLICIT DERIVATION OF ERROR FORMULAS

A. Real-Space Errors

The real-space cutoff error in the force on particle i can be written as¹⁴

$$\Delta \mathbf{F}_i^{(r)} = |\boldsymbol{\mu}_i| \sum_{j \neq i} |\boldsymbol{\mu}_j| \boldsymbol{\chi}_{ij}^{(r)}. \quad (19)$$

The idea behind this is that the error on $\mathbf{F}_i^{(r)}$ originates from the $N - 1$ interactions of particle i with the other dipolar particles, and each contribution should be proportional to the product of the two dipole moments involved. The vector $\boldsymbol{\chi}_{ij}^{(r)}$ gives the direction and magnitude of the error contribution from two unit dipoles in the simulation box, depending on their separation and orientations. It follows from Eqn.(10) that $\boldsymbol{\chi}_{ij}^{(r)}$ is given by

$$\begin{aligned} \boldsymbol{\chi}_{ij}^{(r)} = \sum_{\mathbf{r}, r > r_c} \left\{ [\hat{\mathbf{r}} \cos \vartheta(\hat{\boldsymbol{\mu}}_i, \hat{\boldsymbol{\mu}}_j) + \hat{\boldsymbol{\mu}}_i \cos \vartheta(\hat{\boldsymbol{\mu}}_j, \hat{\mathbf{r}}) + \hat{\boldsymbol{\mu}}_j \cos \vartheta(\hat{\boldsymbol{\mu}}_i, \hat{\mathbf{r}})] r C(r) \right. \\ \left. - \hat{\mathbf{r}} \cos \vartheta(\hat{\boldsymbol{\mu}}_i, \hat{\mathbf{r}}) \cos \vartheta(\hat{\boldsymbol{\mu}}_j, \hat{\mathbf{r}}) r^3 D(r) \right\} \end{aligned} \quad (20)$$

where $\hat{\boldsymbol{\mu}}_i$ and $\hat{\boldsymbol{\mu}}_j$ are unit vectors along the dipole orientations on particles i and j , $\hat{\mathbf{r}}$ is the unit vector along \mathbf{r} , and the sum in (20) runs over all the periodic images of particle j for

$|\mathbf{r} := \mathbf{r}_{ij} + \mathbf{n}| > r_c$. $\vartheta(\hat{\boldsymbol{\mu}}_i, \hat{\boldsymbol{\mu}}_j)$ denotes the angle between the vectors $\hat{\boldsymbol{\mu}}_i$ and $\hat{\boldsymbol{\mu}}_j$, $\vartheta(\hat{\boldsymbol{\mu}}_i, \hat{\mathbf{r}})$ the angle between $\hat{\boldsymbol{\mu}}_i$ and $\hat{\mathbf{r}}$, and so forth.

To derive the estimate of $\Delta \mathbf{F}_i^{(r)}$, we assume that the positions and dipole moment orientations of the particles separated by distances larger than r_c are distributed randomly. This assumption is certainly not valid for all dipolar systems, but it is reasonable as a starting point. For random systems, the error contributions from different particles can be assumed to be uncorrelated¹⁴

$$\langle \boldsymbol{\chi}_{ij}^{(r)} \cdot \boldsymbol{\chi}_{im}^{(r)} \rangle = \delta_{jm} \langle \boldsymbol{\chi}_{ij}^{(r)2} \rangle =: \delta_{jm} \chi^{(r)2}, \quad (21)$$

where the angular brackets denote the average over all particle configurations. Obviously, the term $\langle \boldsymbol{\chi}_{ij}^{(r)2} \rangle$ - the mean square force error for two unit dipoles - can no longer depend on i and j and is thus written as $\chi^{(r)2}$. Using Eqns.(19, 21), it follows that

$$\langle (\Delta \mathbf{F}_i^{(r)})^2 \rangle = \mu_i^2 \sum_{j \neq i} \sum_{m \neq i} |\boldsymbol{\mu}_j| |\boldsymbol{\mu}_m| \langle \boldsymbol{\chi}_{ij}^{(r)} \cdot \boldsymbol{\chi}_{im}^{(r)} \rangle \approx \mu_i^2 \mathcal{M}^2 \chi^{(r)2}, \quad (22)$$

where the quantity \mathcal{M} is defined as

$$\mathcal{M}^2 := \sum_{j=1}^N \mu_j^2. \quad (23)$$

To obtain the configurational average value $\langle \Delta F \rangle$, we further assume that

$$\left\langle \sqrt{\frac{1}{N} \sum_{i=1}^N (\Delta \mathbf{F}_i)^2} \right\rangle \approx \sqrt{\frac{1}{N} \sum_{i=1}^N \langle (\Delta \mathbf{F}_i)^2 \rangle}, \quad (24)$$

which can be shown true for reasonably large systems by the law of large numbers along the line of reasoning of Ref. 14. Inserting Eq.(22) into Eqs.(18, 24) we end up with the relation

$$\Delta F^{(r)} \approx \chi^{(r)} \frac{\mathcal{M}^2}{\sqrt{N}}. \quad (25)$$

Using Eqn.(20), it follows

$$\begin{aligned} \chi^{(r)2} \approx & \frac{1}{L^3} \int_{r_c}^{\infty} r^2 dr \int_0^{\pi} \sin \theta d\theta \int_0^{2\pi} d\phi \left\{ [\hat{\mathbf{r}} \cos \vartheta(\hat{\boldsymbol{\mu}}, \hat{\boldsymbol{\mu}}') + \hat{\boldsymbol{\mu}} \cos \vartheta(\hat{\boldsymbol{\mu}}', \hat{\mathbf{r}}) + \hat{\boldsymbol{\mu}}' \cos \theta] r C(r) \right. \\ & \left. - \hat{\mathbf{r}} \cos \theta \cos \vartheta(\hat{\boldsymbol{\mu}}', \hat{\mathbf{r}}) r^3 D(r) \right\}^2, \end{aligned} \quad (26)$$

where $\hat{\boldsymbol{\mu}}$ and $\hat{\boldsymbol{\mu}}'$ denote the unit orientation vectors of two arbitrary dipoles. The z-axis of the spherical coordinates (r, θ, ϕ) is chosen to be along the orientation $\hat{\boldsymbol{\mu}}$. That gives $\vartheta(\hat{\boldsymbol{\mu}}, \hat{\mathbf{r}}) = \theta$ and

$$\cos \vartheta(\hat{\boldsymbol{\mu}}', \hat{\mathbf{r}}) = \cos \theta \cos \vartheta(\hat{\boldsymbol{\mu}}, \hat{\boldsymbol{\mu}}') + \sin \theta \sin \vartheta(\hat{\boldsymbol{\mu}}, \hat{\boldsymbol{\mu}}') \cos \phi. \quad (27)$$

In the integrand of Eqn.(26), all the triangular functions about $\vartheta(\hat{\boldsymbol{\mu}}, \hat{\boldsymbol{\mu}}')$ should be replaced by their configuration average values. This means that the cross terms which contain odd powers of $\cos / \sin \vartheta(\hat{\boldsymbol{\mu}}, \hat{\boldsymbol{\mu}}')$ will vanish due to their zero mean value. The remaining terms $\cos^2 / \sin^2 \vartheta(\hat{\boldsymbol{\mu}}, \hat{\boldsymbol{\mu}}')$ are replaced by their mean values of 1/2. Following the asymptotic expansion formula¹²

$$\int_A^\infty \exp(-Bx^2) f(x) dx \approx \exp(-BA^2) f(A) / 2BA \quad (28)$$

which is valid when $B > 0$ and $d[f(x)/2Bx]/dx \ll f(x)$ for $x \geq A$, the complementary error function is approximated by

$$\operatorname{erfc}(\alpha r) \approx \exp(-\alpha^2 r^2) / \sqrt{\pi} \alpha r. \quad (29)$$

Eqn.(29) is introduced into (26) through (7, 8). Estimating the integral again with Eqn.(28) gives the approximate expression of $\chi^{(r)2}$. We obtain

$$\chi^{(r)2} \approx L^{-3} r_c^{-9} \alpha^{-4} \left(\frac{13}{6} C_c^2 + \frac{2}{15} D_c^2 - \frac{13}{15} C_c D_c \right) \exp(-2\alpha^2 r_c^2), \quad (30)$$

where the terms C_c and D_c are given by

$$C_c = 4\alpha^4 r_c^4 + 6\alpha^2 r_c^2 + 3, \quad (31)$$

$$D_c = 8\alpha^6 r_c^6 + 20\alpha^4 r_c^4 + 30\alpha^2 r_c^2 + 15. \quad (32)$$

The resulting rms expectation of the real-space cutoff error in the forces is thus

$$\Delta F^{(r)} \approx \mathcal{M}^2 (L^3 \alpha^4 r_c^9 N)^{-1/2} \left(\frac{13}{6} C_c^2 + \frac{2}{15} D_c^2 - \frac{13}{15} C_c D_c \right)^{1/2} \exp(-\alpha^2 r_c^2). \quad (33)$$

The derivation of the expected real-space cutoff errors in the total potential energy and torques follows the same way. For calculating the fluctuation of the error in total energy, it is noted that the interaction energy between two dipoles is evenly shared between them. That means the sum of $\langle (\Delta U^{(r)})^2 \rangle$ over all particles contains each pair contribution twice and thus the fluctuation of the real-space cutoff error is one half of the sum¹². Then the rms value of the real-space cutoff error of the total potential energy is estimated as

$$\Delta U^{(r)} \approx \mathcal{M}^2 (L^3 \alpha^4 r_c^7 N)^{-1/2} \left[\frac{1}{4} B_c^2 + \frac{1}{15} C_c^2 - \frac{1}{6} B_c C_c \right]^{1/2} \exp(-\alpha^2 r_c^2) \quad (34)$$

with

$$B_c = 2\alpha^2 r_c^2 + 1. \quad (35)$$

The rms error on the torques is estimated similarly to the force as

$$\Delta\tau^{(r)} \approx \mathcal{M}^2(L^3\alpha^4r_c^7N)^{-1/2}\left[\frac{1}{2}B_c^2 + \frac{1}{5}C_c^2\right]^{1/2}\exp(-\alpha^2r_c^2). \quad (36)$$

Eqn.(33, 34, 36) all contain the exponential $\exp(-\alpha^2r_c^2)$. For sufficiently low errors, αr_c has to be larger than one, for example $\alpha r_c \approx \pi$ for an error of $\exp(-\pi^2) \approx 5 \times 10^{-5}$. If only the highest powers of αr_c are retained, the estimates of the real-space cutoff errors in the total energy, forces and torques can be reduced to

$$\Delta U^{(r)} \approx 4\mathcal{M}^2\alpha^2(r_c/15NL^3)^{1/2}\exp(-\alpha^2r_c^2), \quad (37)$$

$$\Delta F^{(r)} \approx 8\mathcal{M}^2\alpha^4(2r_c^3/15NL^3)^{1/2}\exp(-\alpha^2r_c^2), \quad (38)$$

$$\Delta\tau^{(r)} \approx 4\mathcal{M}^2\alpha^2(r_c/5NL^3)^{1/2}\exp(-\alpha^2r_c^2), \quad (39)$$

where Eqn.(37) is a factor of $\sqrt{6/5}$ slightly larger than that given in Eqn.(35) of Ref. 12. The advantage of these simplified formulas is that they reflect the dependence of the rms errors on α and r_c more directly and thus could be used more easily in determining the optimal values of these parameters.

B. Reciprocal-Space Errors

In deriving the estimates of the reciprocal-space (k-space) cutoff errors, we further assume that the radial distribution function of the particles is approximately unity at all distances. Following Eqn.(11), the k-space cutoff error in the force acting on particle i is given by

$$\Delta\mathbf{F}_i^{(k)} = \sum_{j=1}^N \sum_{\mathbf{k}, k > k_c} \frac{8\pi^2\mathbf{k}}{L^4k^2} (\boldsymbol{\mu}_i \cdot \mathbf{k})(\boldsymbol{\mu}_j \cdot \mathbf{k}) \exp[-(\pi k/\alpha L)^2] \sin(2\pi\mathbf{k} \cdot \mathbf{r}_{ij}/L). \quad (40)$$

Note that the diagonal term ($j = i$) in the sum does not depend on the positions of the particles. It will provide a systematic contribution to the cutoff error in k-space¹². In Eqn.(40) this contribution equals to zero, thus there is no systematic part of the error in the forces. The same thing happens to the error in the torques. But for the total energy the diagonal terms are positive and the systematic contribution plays a dominant role in the cutoff error.

The off-diagonal terms in Eqn.(40) do depend on the positions of the particles and have alternating signs. The statistical approach in Sec. III.A can also be used. Similar to Eqn.(19), the off-diagonal contribution to the cutoff error in $\Delta\mathbf{F}_i^{(k)}$ is given by

$$\Delta\mathbf{F}_{i,off}^{(k)} = |\boldsymbol{\mu}_i| \sum_{j \neq i} |\boldsymbol{\mu}_j| \boldsymbol{\chi}_{ij}^{(k)} \quad (41)$$

with

$$\boldsymbol{\chi}_{ij}^{(k)} = \sum_{\mathbf{k}, k > k_c} \frac{8\pi^2\mathbf{k}}{L^4} \cos\vartheta(\hat{\boldsymbol{\mu}}_i, \hat{\mathbf{k}}) \cos\vartheta(\hat{\boldsymbol{\mu}}_j, \hat{\mathbf{k}}) \exp[-(\pi k/\alpha L)^2] i \exp(2\pi i\mathbf{k} \cdot \mathbf{r}/L), \quad (42)$$

where \mathbf{r} stands for \mathbf{r}_{ij} and $\sin(2\pi\mathbf{k} \cdot \mathbf{r}/L)$ is re-written as $i \exp(2\pi i\mathbf{k} \cdot \mathbf{r}/L)$ according to the symmetrical character of the summation over \mathbf{k} . $\hat{\mathbf{k}}$ is the unit vector along \mathbf{k} . Since the particles are assumed to be randomly distributed over the simulation box, the fluctuation of $\Delta\mathbf{F}_{i,off}^{(k)}$ can also be written as

$$\left\langle (\Delta\mathbf{F}_{i,off}^{(k)})^2 \right\rangle = \mu_i^2 \sum_{j \neq i} \sum_{m \neq i} |\boldsymbol{\mu}_j| |\boldsymbol{\mu}_m| \langle \boldsymbol{\chi}_{ij}^{(k)} \cdot \boldsymbol{\chi}_{im}^{(k)*} \rangle \approx \mu_i^2 \mathcal{M}^2 \chi^{(k)2}. \quad (43)$$

Again $\chi^{(k)2}$ is independent of i and j . Using Eqn.(42), we have

$$\chi^{(k)2} \approx \left(\frac{8\pi^2}{L^4} \right)^2 \int_{k_c}^{\infty} \exp[-2(\pi k/\alpha L)^2] k^4 dk \int_0^{\pi} \sin \theta d\theta \int_0^{2\pi} \cos^2 \vartheta(\hat{\boldsymbol{\mu}}, \hat{\mathbf{k}}) \cos^2 \vartheta(\hat{\boldsymbol{\mu}}', \hat{\mathbf{k}}) d\phi. \quad (44)$$

Choosing the z-axis of the spherical coordinates (k, θ, ϕ) along the $\hat{\boldsymbol{\mu}}$ orientation, the same discussion as in Eqn.(26) gives

$$\chi^{(k)2} \approx 128\pi^3 L^{-6} \alpha^2 k_c^3 \exp[-2(\pi k_c/\alpha L)^2]/15. \quad (45)$$

The rms expectation of the k-space cutoff error in the forces is thus

$$\Delta F^{(k)} \approx 8\pi \mathcal{M}^2 L^{-3} \alpha (2\pi k_c^3/15N)^{1/2} \exp[-(\pi k_c/\alpha L)^2]. \quad (46)$$

Here the notation $\Delta F_{off}^{(k)}$ is replaced directly with $\Delta F^{(k)}$ due to the fact of no diagonal contribution.

The derivation of the off-diagonal parts of the cutoff errors in the total energy and torques proceeds in the same way. That the sum over $\langle (\Delta U_{i,off}^{(k)})^2 \rangle$ contains each pair contribution twice has also been considered in the error estimate of the total energy. The results are given by

$$\Delta U_{off}^{(k)} \approx 4\mathcal{M}^2 L^{-2} \alpha (\pi k_c/15N)^{1/2} \exp[-(\pi k_c/\alpha L)^2], \quad (47)$$

$$\Delta \tau^{(k)} \approx 4\mathcal{M}^2 L^{-2} \alpha (\pi k_c/5N)^{1/2} \exp[-(\pi k_c/\alpha L)^2]. \quad (48)$$

$\Delta \tau^{(k)}$ is also used directly instead of $\Delta \tau_{off}^{(k)}$.

The diagonal (systematic) part of the cutoff error in the total energy can be written as

$$\begin{aligned} \Delta U_{diag}^{(k)} &= \frac{1}{2\sqrt{N}} \sum_{i=1}^N \sum_{\mathbf{k}, k > k_c} \frac{4\pi}{L^3} \mu_i^2 \cos^2 \vartheta(\hat{\boldsymbol{\mu}}_i, \hat{\mathbf{k}}) \exp[-(\pi k/\alpha L)^2] \\ &\approx \frac{2\pi}{L^3 \sqrt{N}} \mathcal{M}^2 \int_{k_c}^{\infty} \exp[-(\pi k/\alpha L)^2] k^2 dk \int_0^{\pi} \sin \theta d\theta \int_0^{2\pi} \cos^2 \vartheta(\hat{\boldsymbol{\mu}}, \hat{\mathbf{k}}) d\phi \\ &\approx \frac{4}{3} \mathcal{M}^2 L^{-1} \alpha^2 k_c N^{-1/2} \exp[-(\pi k_c/\alpha L)^2], \end{aligned} \quad (49)$$

where the sum is again approximated by an integral and the asymptotic expansion formula of Eqn.(28) is used to get the final estimate. The total k-space cutoff error in the total energy is thus

$$\Delta U^{(k)} = \Delta U_{diag}^{(k)} + \Delta U_{off}^{(k)}. \quad (50)$$

Comparing Eqn.(49) with (47), it can be seen that the systematic part of the error is a factor of $\sim L\alpha k_c^{1/2} (\gg 1)$ larger than the statistical part. Hence the systematic contribution is dominant in the k-space cutoff error of the total energy.

Assuming that the real-space and reciprocal-space contributions to the error are independent, the total cutoff error in Ewald summation can be written as

$$\Delta\Theta = \sqrt{\Delta\Theta^{(r)2} + \Delta\Theta^{(k)2}}, \quad (51)$$

where Θ stands for U, F and τ .

IV. COMPARISON OF FORMULA WITH NUMERICAL CALCULATION

In this section, we carry out numerical experiments to check the validity of the error estimates derived in the previous section.

In order to make our measurements fully reproducible, we choose the test system to be consistent with the one described in Appendix D of a previous publication:¹⁰ 100 particles randomly distributed within a cubic box of length $L = 10$, each of them has a unit point-dipole at the center. The coordinates and dipole orientations of the 100 particles are constructed by generating 500 random numbers \mathcal{R}_n ($n = 1, \dots, 500$) between 0 and 1. The first 300 random numbers give the Cartesian coordinates of the particles as ($x_i = L\mathcal{R}_{3i-2}, y_i = L\mathcal{R}_{3i-1}, z_i = L\mathcal{R}_{3i}$). The remaining 200 numbers distribute the dipole orientations uniformly over a unit sphere's surface by the following way:

$$\cos\theta_i = 2\mathcal{R}_{300+2i-1} - 1.0, \quad (52)$$

$$\phi_i = 2\pi\mathcal{R}_{300+2i}, \quad (53)$$

yielding ($\hat{\boldsymbol{\mu}}_{ix} = \sin\theta_i \cos\phi_i, \hat{\boldsymbol{\mu}}_{iy} = \sin\theta_i \sin\phi_i, \hat{\boldsymbol{\mu}}_{iz} = \cos\theta_i$). The function `rand` which can be found in many `C` libraries is used as the random number generator. Thus the positions of the particles are exactly the same as that discussed in Refs. 10,14. Our unit conventions are as follows: lengths are measured in \mathcal{L} and dipoles in \mathcal{P} . Hence the unit of the energy, force and torque are $\mathcal{P}^2/\mathcal{L}^3, \mathcal{P}^2/\mathcal{L}^4$ and $\mathcal{P}^2/\mathcal{L}^3$, respectively.

The *exact* energy, forces and torques are obtained by performing a direct summation in real space with Eqn.(1) and the related derivatives. The sum over \mathbf{n} is built up in a spherical way up to $|\mathbf{n}_{cut}| = 40L$. The Ewald summation calculations are carried out under vacuum condition ($\epsilon' = 1$) in order to compare the results with the direct summation^{16,17}. The rms errors in the forces and torques are evaluated directly with the definition of Eqn.(18). However, it is inconvenient to do this for the energy due to the existence of the constant contributions ($U^{(self)}$ and $U^{(surf)}$), so the rms error in the total energy is simply taken as

$$\Delta U = \langle (U - U^{exa})^2 \rangle^{1/2}, \quad (54)$$

where the angular brackets denote the configuration average. If only one specific random system is considered, the use of Eqn.(54) may make the result on ΔU somewhat sensitive to the details of the generated configuration. But it is easy to see that this sensitivity can be diminished by taking an average over several configurations.

In the first step, we fix the real-space cutoff to $r_c = 5.0 (L/2)$. The k-space cutoff k_c changes from 2 to 12. The resulting curves for the rms errors in the forces and torques are plotted in Fig.1(a) and (b) together with the analytical estimates derived in Sec. III. To avoid the unfavorable sensitivity to configuration details, the result on the rms error of the total energy [Fig.1(c)] is taken from an average over 10 random configurations which are generated one after the other in the same way as the model system. Fig.1(a-c) show that for each k_c there exists an optimal value of α which gives the minimum rms errors. For smaller values of α , the error contribution from the real-space is dominant, while for larger values the k-space contribution dominates. It can be clearly seen that the analytical estimates accurately predict both the real-space and k-space contributions to ΔF , $\Delta\tau$ and ΔU for all values of α . Only for very small values of k_c deviations are observed for large α . As will be shown in the next section, this permits an easy way to determine the optimal parameters for a predefined accuracy. The discrepancy in the k-space part at very low k_c is to be expected as the replacement of the summation over \mathbf{k} with an integral in Eqn.(44) turns to be a rather crude approximation at this time. Since the optimal values of k_c for the Ewald method are ranging between 7 and 25¹³, this discrepancy does not affect the validity of the analytical estimates. As accuracy on the energy may be obscured by unimportant constant contributions and is sensitive to fluctuations, the rms errors on the forces and torques are more suitable for the accuracy measurements in MD simulations. Furthermore, since Fig.1(a, b) show the similar behavior of ΔF and $\Delta\tau$ as function of α and k_c (for example, they give the same optimal value of α for each k_c), we will concentrate on discussions of ΔF in the remaining part of this paper. The same kind of results, however, have been achieved for ΔU and $\Delta\tau$ in all the following cases.

As most discussions are focused on the k-space error contributions in Fig.1 by changing k_c , we fix k_c in the next step and change different values for r_c in order to further investigate the accuracy of the analytical estimates in predicting the real-space error contributions. The same model system as in Fig.1(a, b) is studied. k_c is fixed to 8 and r_c is taken to be 3.0, 3.6, 4.3 and 5.0, respectively. For comparison, both Eqn.(33) and (38) are used to estimate $\Delta F^{(r)}$. The results in Fig.2 show that the former formula precisely gives the real-space contribution to ΔF for all values of r_c . As expected, Eqn.(38) underestimates $\Delta F^{(r)}$ at small values of α . Since Eqns.(37-39) are obtained under the assumption of $\alpha r_c \gg 1$, the valid range of these simplified formulas shifts to larger α with decrease of r_c . However, if an accuracy as $\delta \leq 5 \times 10^{-5}$ is required in a MD simulation so that α could not be very small considering the practical limitation of $r_c \leq L/2$, these estimates are almost as accurate as the full formulas [Eqns.(33), (34) and (36)].

The last step is to demonstrate that the scaling of the rms errors with the particle number and dipole moment distribution is correctly given by $\Delta F \propto \mathcal{M}^2 N^{-1/2}$. Three random systems which differ only in the values of \mathcal{M}^2 and N are investigated. The first system is the same as that studied in Fig.1-2. The second system contains 200 particles among which 100 have a dipole strength of \mathcal{P} and the other 100 have $3\mathcal{P}$. The third one

contains 400 particles: 100 with \mathcal{P} , 200 with $5\mathcal{P}$ and 100 with $7\mathcal{P}$. Hence their values of (\mathcal{M}^2, N) are respectively given by (100, 100), (1000, 200) and (10000, 400), and the ratio of their prefactors is thus $1 : \sqrt{50} : 50$. The results of ΔF in Fig.3 clearly reflect this scaling behavior by the constant shift of the three curves with respect to each other (note the logarithmic scale in the vertical axis). The analytical estimates predict the rms errors very precisely in all the three cases.

V. OPTIMIZATION OF PARAMETERS

In this section, we discuss the use of the analytical formulas derived in Sec. III to determine the optimal values of α , r_c and k_c by which the required accuracy could be satisfied and the computation time is minimized. The detailed discussions on this subject can also be found in Refs. 6,13.

The overall computation time for computing the forces with the Ewald method is approximately given by¹³

$$\mathcal{T} = a_r N^2 (r_c/L)^3 + a_k N k_c^3, \quad (55)$$

where the primitive overheads a_r and a_k highly depend on the implementation of the code and need to be found by numerical experiments. As an example, we have carried out the time experiments on a DEC personal workstation (CPU 433MHz) using a standard Fortran 77 compiler. In the implementation the complementary error function and its derivative are calculated with table lookup and the reciprocal-space summation is optimized as in Refs. 6,15. The linked-cell method is used to deal with the short-range forces (when doing simulations). The primitive overheads are then found roughly to be $a_r = 2.5\mu s$ and $a_k = 0.7\mu s$.

For a required accuracy δ , the parameters α , r_c and k_c should be chosen to minimize \mathcal{T} with respect to the two constraints of the error bounds [Eqns.(33) and (46)], which are restated as

$$\frac{\delta}{\sqrt{2}} = \mathcal{M}^2 (L^3 \alpha^4 r_c^9 N)^{-1/2} \left(\frac{13}{6} C_c^2 + \frac{2}{15} D_c^2 - \frac{13}{15} C_c D_c \right)^{1/2} \exp(-\alpha^2 r_c^2), \quad (56)$$

$$\frac{\delta}{\sqrt{2}} = 8\pi \mathcal{M}^2 L^{-3} \alpha (2\pi k_c^3 / 15N)^{1/2} \exp[-(\pi k_c / \alpha L)^2]. \quad (57)$$

In case of $\delta \leq 5 \times 10^{-5}$, Eqn.(38) could be used instead of (33) so as to show the dependence of the accuracy on the parameters more clearly. Eqn.(56) and (57) provide the qualitative function relations of r_c and k_c with α as: $r_c(\alpha) \approx -A\sqrt{\ln \delta}/\alpha$ and $k_c(\alpha) \approx -B\sqrt{\ln \delta}\alpha$. Inserting them into Eqn.(55) and differentiating it with respect to α yields $\alpha \propto N^{1/6}$ and thus $r_c \propto N^{-1/6}$ and $k_c \propto N^{1/6}$. The minimized computation time is then proportional to $N^{3/2}$ with the proportionality constant depending on the accuracy. The same results can be found for the Coulomb Ewald method in Refs. 6,12,13. This can be easily understood by comparing Eqns.(33) and (46) in Sec. III of this paper with Eqns.(18) and (32) in Ref. 12 and finding the same exponential dependences of the cutoff errors on α , r_c and k_c for the dipolar and Coulomb Ewald summations.

The numerical investigation of the functional dependence of the optimal parameters on N and δ are performed by using the primitive overheads obtained above. For each given N and δ , we at first choose different values for r_c within the inequality $r_c \leq L/2$. For each r_c the parameters α and k_c are calculated by solving Eqns.(56) and (57). These values are then introduced into Eqn.(55) to figure out the optimal value of r_c which gives the minimum computation time. In calculations the size of the simulation cell is fixed to a dimensionless length of $L = 10$. The range of accuracy requirement and number of particles are chosen to be $\delta = 10^{-2}$ to 10^{-5} measuring in $\mathcal{P}^2/\mathcal{L}^4$ and $N = 10^3$ to $N = 10^6$ which should cover most of the applications. The particles are supposed to have an uniform dipole moment of \mathcal{P} . The results for the optimal values of the parameters and the corresponding computation time per particle are shown in Fig. 4(a-d), respectively. It can be clearly seen that the functional dependence of the parameters and the overall computation time on N are just as discussed above. Fig.4(c) shows that when a high accuracy is required for a system with a small number of particles, the predicted real-space cutoff is larger than half of the box length and $r_c = L/2$ must be used. The optimal α values hardly depend on the accuracies. These results are very similar to that obtained for the Coulomb Ewald summation in Ref. 13, except for $r_c \propto N^{-1/6}$ here and $r_c \propto N^{1/6}$ there. This is because they considered a system of constant density, while we choose the volume of the simulation cell to be constant.

VI. APPLICATION TO AN INHOMOGENEOUS SYSTEM

So far we have only used the homogeneous random systems to test the error estimates. This is of course not always the case in computer experiments. Many simulations will encounter the problem of highly nonuniform distributions of particles. In this section we use an anisotropic dipolar system to investigate the influence of the inhomogeneity on the rms errors.

The dipolar system we studied is an electrorheological (ER) fluid consisting of spherical dielectric particles with uniform diameter σ dispersed in a solvent. In the initial configuration 200 particles are randomly distributed in a cubic simulation box with side length of 10σ , which gives a typical volume fraction of particles as $\rho \approx 0.1$. Upon application of an external electric field, the dielectric particles are polarized. Each particle has an uniform dipole moment along the field direction (z-axis) at its center under the 'point-dipole' approximation. The electrostatic interaction between the particles will draw them to form chain or cluster structures along the field direction. This structuring process of the ER system in the quiescent state is studied by the Brownian dynamic simulation method described in our previous paper¹⁸. The final configuration, which is used for the rms error calculation, is obtained after a long enough simulation time when there is no obvious structure evolution in the system. The formation of several thick chain-like structures has been observed in the snapshot of the system. It is also reflected clearly by the appearance of the sharp peaks at the positions of $r = \sigma, \sqrt{3}\sigma, 2\sigma, \sqrt{7}\sigma, 3\sigma \dots$ in the radial distribution function (RDF) $g_0(r)$ of the final configuration shown in Fig.5, where the RDF of the initial configuration is also plotted for comparison. The rms force error ΔF and the corresponding estimates [Eqns.(33) and (46)] for the final configuration are given in Fig.6. A deviation of the estimates from the numerical results could be observed. At smaller values of α the prediction of the estimates is smaller than that given by the algorithm, while at large values of α it is larger than the

actual one. By studying the derivation of the error estimates, this could be understood qualitatively by the reason that the formation of the chain structures leads to higher local density of the particles and thus results in higher rms errors in the real-space part¹³. Though this effect also exists in the k-space part, the well ordering, or in other word well spacing, of particles along the z-direction leads to an enhanced k-space accuracy. This could be partially seen from Eqn.(11) where only the z-component k_z involves in the calculation due to the z-direction orientation of the dipole moments in this case.

From the numerical curve in Fig.6, the optimal splitting parameter is given to be $\alpha \approx 0.72\sigma^{-1}$ with a corresponding $\Delta F \approx 1.74 \times 10^{-5}$, while the intersection point of the real and reciprocal space estimates occurs at $\alpha \approx 0.71\sigma^{-1}$, which predicts an error of $\Delta F \approx 1.90 \times 10^{-5}$ by Eqn.(56) and (57). If the estimated value of α is used, this would result in an error of $\Delta F \approx 1.88 \times 10^{-5}$, which is about 8% larger than that at the calculated optimal value of α . If such a safety margin has already been considered at the beginning of the simulation, the determination of the optimal parameters discussed in the previous section is still a good approach. In addition, it should be noted that the structure studied in Fig.6 is an extreme case in the simulations of ER fluids or similar systems such as magnetorheological (MR) fluids and ferrofluids. When the thermal agitation is comparable with the dipolar interactions, or even more a shear flow is introduced, the percolating chains or columns will be broken into clusters. The distribution and orientation of the smaller clusters would have more random characters compared with that studied in this section, and thus a smaller discrepancy between the estimates and actual numerical results could be expected. In any case, if it is suspected that the development of strongly inhomogeneities in the systems may lead to potential failure of the presented error formulas, some simple numerical tests as performed above could provide valuable informations.

VII. CONCLUSION

The analytical formulas for the cutoff errors in the Ewald summation for dipolar systems have been derived in closed form. Errors in the total energy, forces and torques are all considered. The high quality of these estimates has been proven in different random systems, and thus provides an easy way to determine the optimal tuning parameters which can give the expected accuracy, but minimize the computation time. Based on this, the functional dependence of the optimal splitting parameter α , real-space cutoff r_c and reciprocal-space cutoff k_c on the number of particles N are discussed qualitatively and confirmed numerically by the timing experiments. Although the validity of the error estimates is subject to some additional requirements, such as the homogeneity of the system, a consultation of these formulas and a priori estimate of the optimal parameters should always be a good starting point in using the Ewald summation for simulations of dipolar systems.

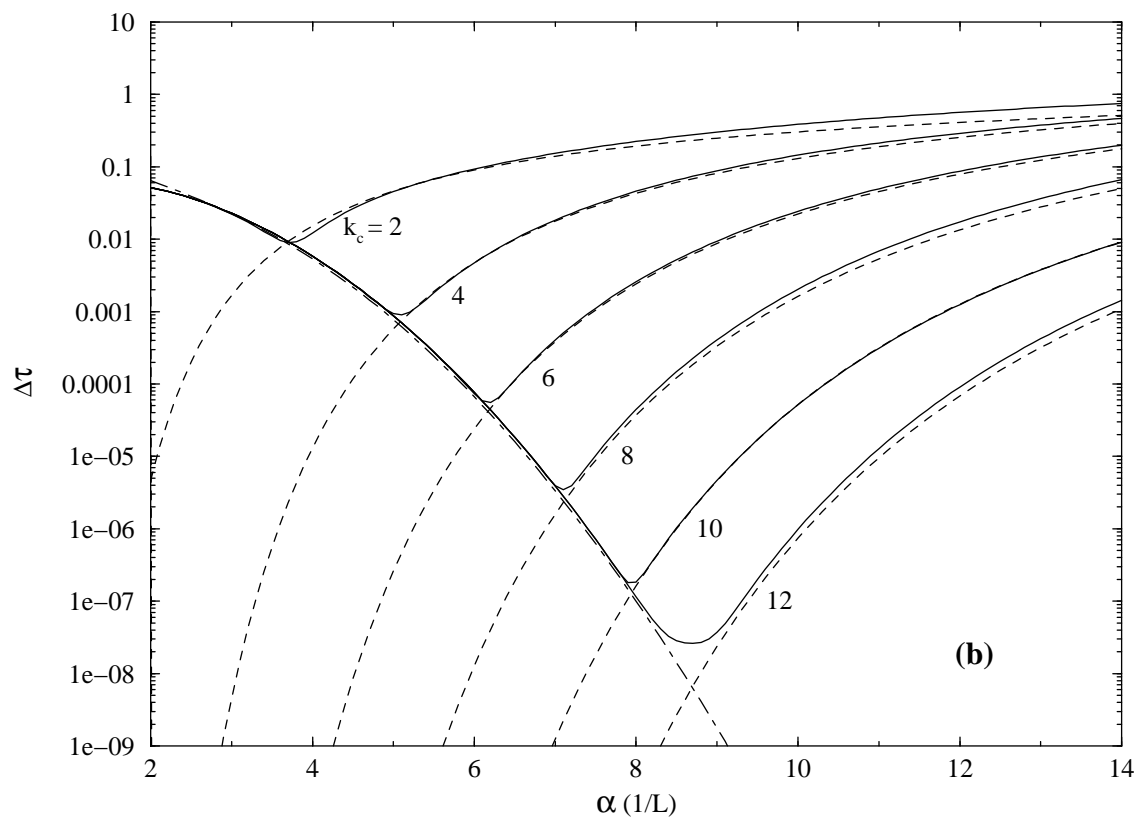
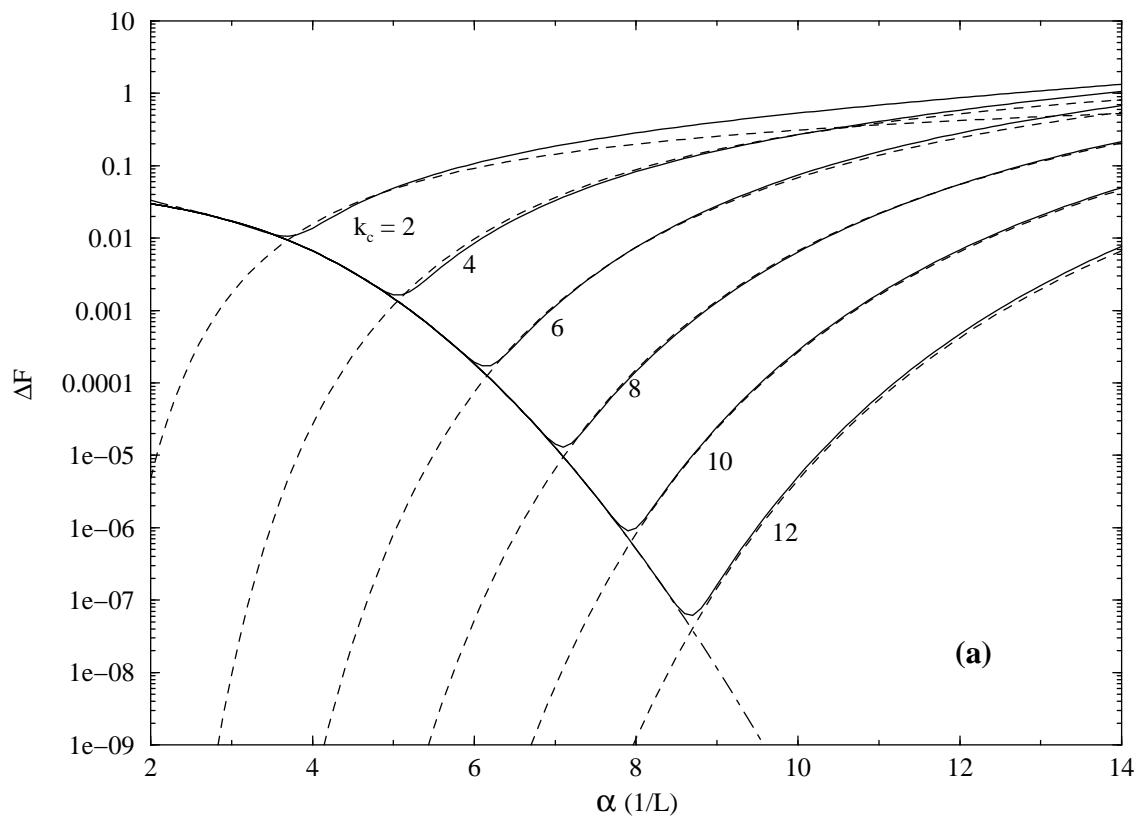
VIII. ACKNOWLEDGMENTS

We thank H. W. Müller and B. Dünweg for helpful discussions. Financial support from the DFG is gratefully acknowledged.

REFERENCES

- ¹ *Electrostatic Effects in Soft Matter and Biophysics*, *Nato Science Series*, edited by C. Holm, P. Kékicheff, and R. Podgornik (Kluwer, Dordrecht, to be published).
- ² *Polyelectrolytes: Science and Technology*, edited by M. Hara (Marcel Dekker, New York, 1993).
- ³ X. Daura, A. Mark, and W. van Gunsteren, *Computer Physics Communications* **123**, 97 (1999).
- ⁴ R. E. Rosensweig, *Ferrohydrodynamics* (Cambridge Univ. Press, Cambridge, 1985).
- ⁵ P. Ewald, *Ann. Phys.* **64**, 253 (1921).
- ⁶ J. Perram, H. G. Petersen, and S. de Leeuw, *Mol. Phys.* **65**, 875 (1988).
- ⁷ R. W. Hockney and J. W. Eastwood, *Computer Simulation Using Particles* (IOP, London, 1988).
- ⁸ D. Y. T. Darden and L. Pedersen, *J. Chem. Phys.* **98**, 10089 (1993).
- ⁹ U. Essmann *et al.*, *J. Chem. Phys.* **103**, 8577 (1995).
- ¹⁰ M. Deserno and C. Holm, *J. Chem. Phys.* **109**, 7678 (1998).
- ¹¹ P. H. Hünenberger, *J. Chem. Phys.* **113**, 10464 (2000).
- ¹² J. Kolafa and J. W. Perram, *Molecular Simulation* **9**, 351 (1992).
- ¹³ H. G. Petersen, *J. Chem. Phys.* **103**, 3668 (1995).
- ¹⁴ M. Deserno and C. Holm, *J. Chem. Phys.* **109**, 7694 (1998).
- ¹⁵ M. P. Allen and D. J. Tildesley, *Computer Simulation of Liquids*, *Oxford Science Publications*, 1 ed. (Clarendon Press, Oxford, 1987).
- ¹⁶ S. W. De Leeuw, J. W. Perram, and E. R. Smith, *Proc. R. Soc. Lond. A* **373**, 27 (1980).
- ¹⁷ T. M. Nyman and P. Linse, *J. Chem. Phys.* **112**, 6152 (2000).
- ¹⁸ Z. W. Wang, H. P. Fang, Z. F. Lin, and L. W. Zhou, *Phys. Rev. E* **61**, 6837 (2000).

FIGURES



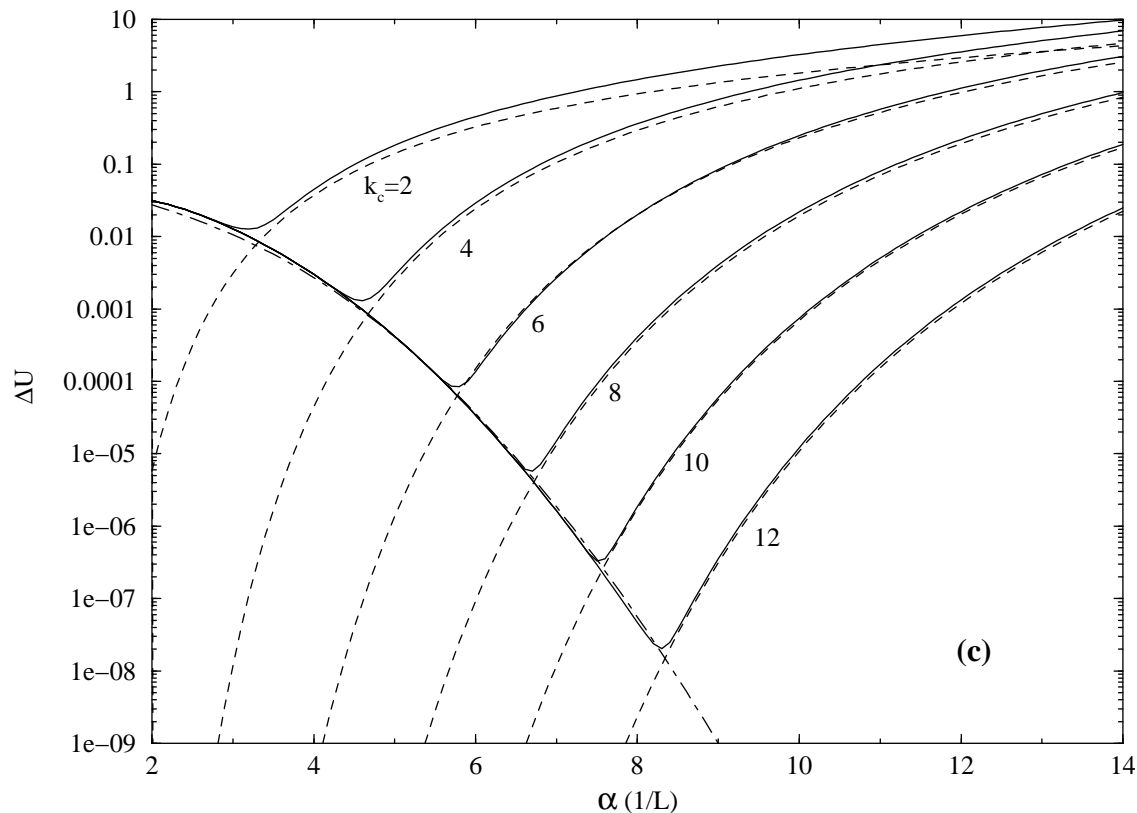


FIG. 1. The rms errors (solid lines) on the forces ΔF (a), torques $\Delta\tau$ (b) and total energy ΔU (c) as a function of the splitting parameter α . The results on ΔF and $\Delta\tau$ are obtained for the model system of 100 randomly distributed dipoles, while ΔU is calculated from an average over 10 random configurations which are generated in the same way as the model system. The real-space cutoff is taken to be $r_c = 5.0$. The dot-dashed curves are the corresponding real-space error estimates achieved with Eqn.(33, 36) and (34). The dashed curves are the k-space error estimates obtained with Eqn.(46, 48) and (50). The units of the energy, force and torque are $\mathcal{P}^2/\mathcal{L}^3$, $\mathcal{P}^2/\mathcal{L}^4$ and $\mathcal{P}^2/\mathcal{L}^3$, respectively.

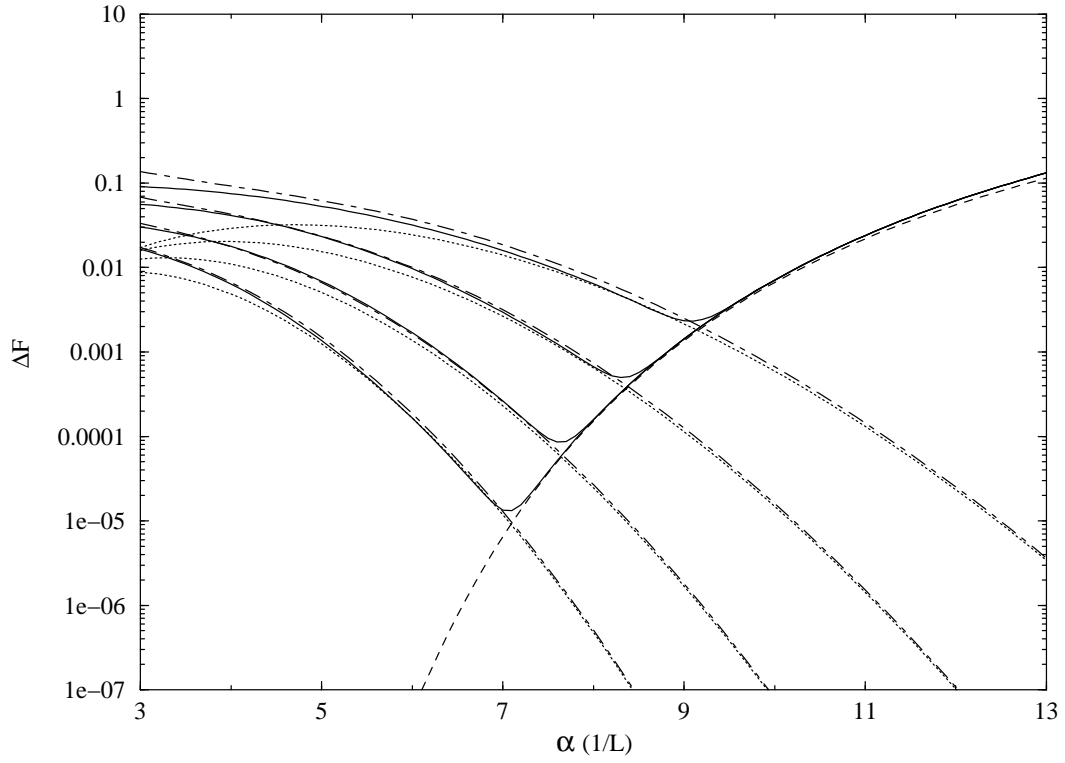


FIG. 2. The rms errors (solid lines) in the forces ΔF for the model system. The k-space cutoff is taken to be $k_c = 8$. From top to bottom the real-space cutoff varies like $r_c = 3.0, 3.6, 4.3, 5.0$. The dot-dashed curves are the corresponding real-space error estimates achieved with Eqn.(33). The results obtained with the simplified formula Eqn.(38) (the dotted curves) are also shown for comparison. The dashed curves are the k-space error estimates obtained with Eqn.(46). The unit of the force is $\mathcal{P}^2/\mathcal{L}^4$.

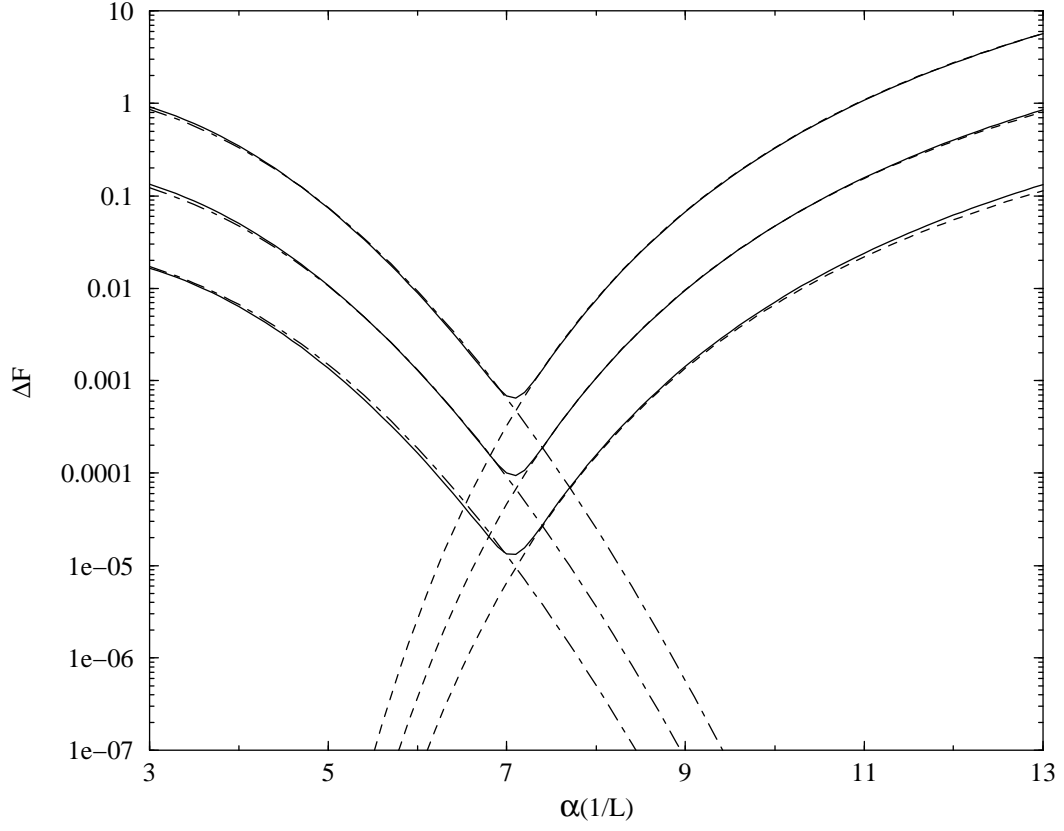


FIG. 3. Test of the $\mathcal{M}^2 N^{-1/2}$ scaling of ΔF . The three solid lines show the rms error ΔF for systems which are different in their (\mathcal{M}^2, N) values. From top to bottom they are characterized by $(10000, 400)$, $(1000, 200)$ and $(100, 100)$ (the last one is the model system discussed in Fig.(1-2)). The real and k-space cutoffs are $r_c = 5.0$ and $k_c = 8$, respectively. The dot-dashed and dashed curves are the corresponding real-space and k-space error estimates obtained with Eqn.(33) and (46), respectively. The unit of the force is $\mathcal{P}^2/\mathcal{L}^4$.

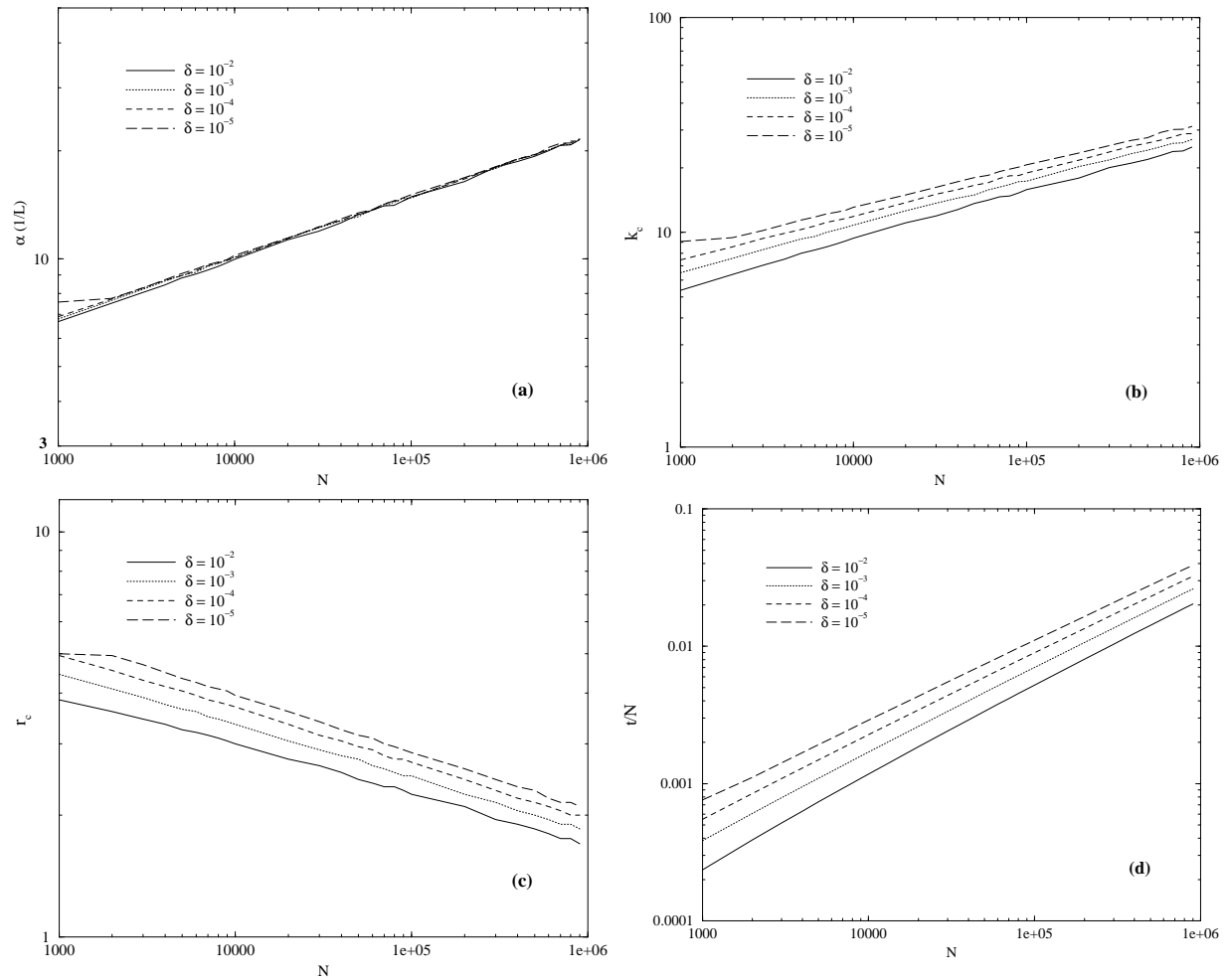


FIG. 4. Optimal values of the parameters α (a), k_c (b) and r_c (c) as well as the corresponding minimized computation time \mathcal{T}/N (d) as a function of the number of particles.

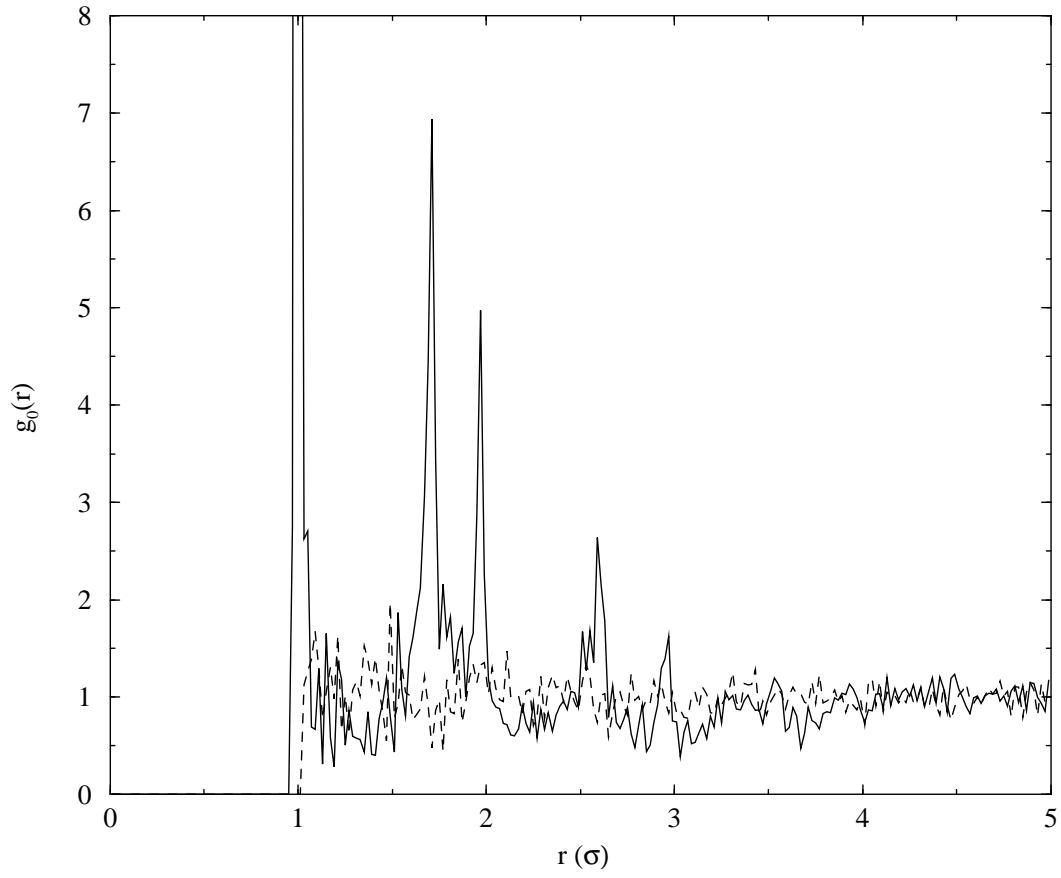


FIG. 5. The radial distribution function (RDF) of the initial (dashed line) and final (solid line) configurations of the electrorheological system studied. The sharp peaks in the RDF of the final configuration reflect the formation of chain-like structures along the field direction.

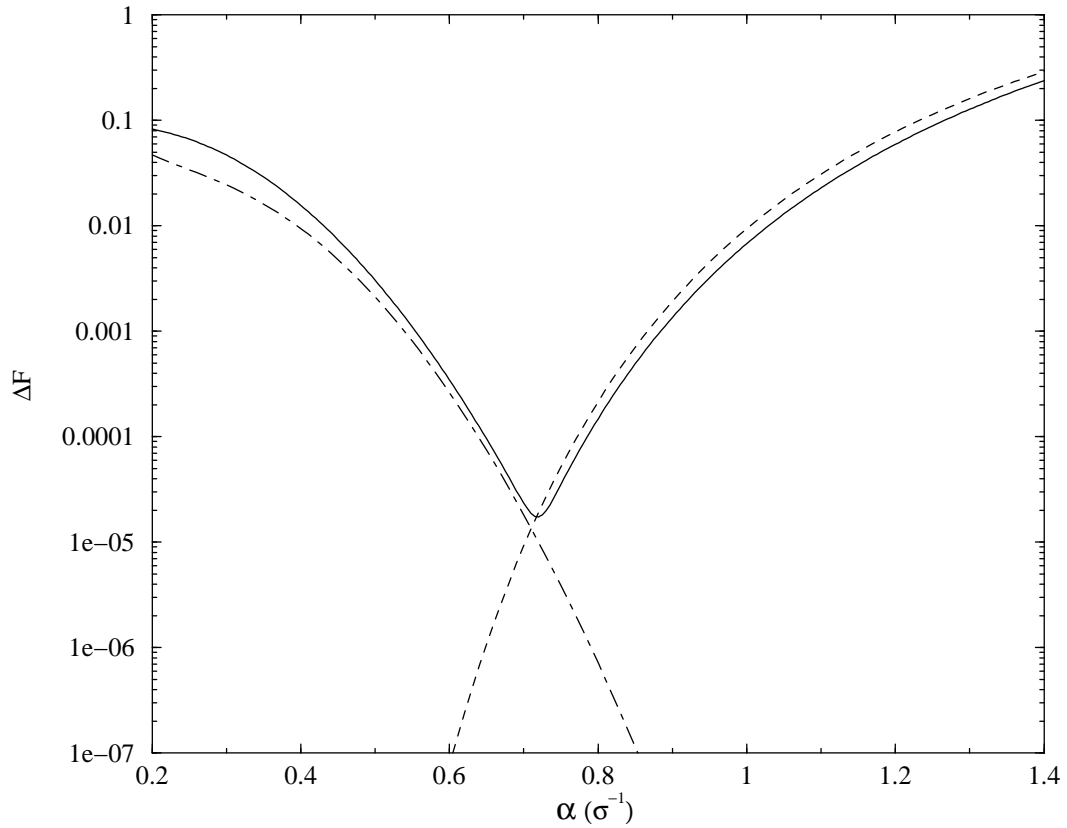


FIG. 6. The rms force error ΔF for the final structure of the electrorheological system studied (solid line). The dot-dashed line is the error estimate for the real-space contribution [Eqn.(33)] and the dashed line is that for the k-space [Eqn.(46)]. The unit of the force is \mathcal{P}^2/σ^4 .